



# Stress analysis and material tailoring in isotropic linear thermoelastic incompressible functionally graded rotating disks of variable thickness

G.J. Nie<sup>a</sup>, R.C. Batra<sup>b,\*</sup>

<sup>a</sup> School of Aerospace Engineering and Applied Mechanics, Tongji University, Shanghai 200092, China

<sup>b</sup> Department of Engineering Science and Mechanics, M/C 0219, Virginia Polytechnic Institute and State University, Blacksburg, VA 24061, USA

## ARTICLE INFO

### Article history:

Available online 13 September 2009

### Keywords:

Rotating disk  
Variable thickness  
Material tailoring  
Functionally graded rubberlike materials  
Thermal stress

## ABSTRACT

We analyze axisymmetric deformations of a rotating disk with its thickness, mass density, thermal expansion coefficient and shear modulus varying in the radial direction. The disk is made of a rubberlike material that is modeled as isotropic, linear thermoelastic and incompressible. We note that the hydrostatic pressure in the constitutive relation of the material is to be determined as a part of the solution of the problem since it cannot be determined from the strain field. The problem is analyzed by using an Airy stress function  $\varphi$ . The non-homogeneous ordinary differential equation with variable coefficients for  $\varphi$  is solved either analytically or numerically by the differential quadrature method. We have also analyzed the challenging problem of tailoring the variation of either the shear modulus or the thermal expansion coefficient in the radial direction so that a linear combination of the hoop stress and the radial stress is constant in the disk. For a rotating annular disk we present the explicit expression of the thermal expansion coefficient for the hoop stress to be uniform within the disk. For a rotating solid disk we give the exact expressions for the shear modulus and the thermal expansion coefficient as functions of the radial coordinate so as to achieve constant hoop stress. Numerical results for a few typical problems are presented to illuminate effects of material inhomogeneities on deformations of a hollow and a solid rotating disk.

© 2009 Elsevier Ltd. All rights reserved.

## 1. Introduction

Functionally graded materials (FGMs) are composites in which the volume fraction, sizes, and shapes of material constituents can be varied to get desired smooth spatial variations of macroscopic properties such as the elastic modulus, the mass density, the heat conductivity, etc. to optimize their performance. The FGMs abound in nature, e.g., human teeth, bamboo stick, sea shell. Engineered FGMs include ceramic–metal and fiber-reinforced polymeric composites, concrete, and rubberlike materials [1–5]. Vulcanized rubber components typically exhibit a spatial variation of mechanical properties caused either by thermal gradients during their fabrication or chemical changes induced due to interaction with the environment during their service [6–8]. For example, in a commercial butyl rubber sheet and a chlorosulfonated polyethylene cable jacketing material the shear modulus was found to be a quadratic function of the radius [9]. Note that during the fabrication (vulcanization) of thick rubber parts the central portion is cured less than the material near the boundary surfaces

unless the vulcanization time is sufficiently large [8,9]. Thus the shear modulus at the center is less than that at the surfaces.

Rubberlike materials are widely used in aerospace, automotive, and biomedical fields. They are usually regarded as incompressible, can thus undergo only isochoric or volume preserving deformations, and their constitutive relation involves hydrostatic pressure that cannot be determined from the deformation field but is to be found as a part of the solution of the boundary-value problem (BVP). The BVPs for functionally graded incompressible materials (FGIMs) are challenging since the governing differential equations have variable coefficients and it is difficult to find their exact solutions. In general, the solution of a BVP for a structure composed of an FGIM cannot be obtained from that of the corresponding problem for a compressible material by setting Poisson's ratio equal to 0.5. Furthermore, the solution for a plane stress problem cannot be obtained from that for a plane strain problem by modifying Young's modulus  $E$  and Poisson's ratio  $\nu$ . We briefly review below the literature on FG rotating disks and other works for FGIMs.

Deformations of a rotating disk composed of a linear elastic, isotropic and homogeneous material have been studied thoroughly [10] and those of a FG rotating disk have been investigated by Horgan and Chan [11] by assuming that  $E$  is a power-law function of the radius  $r$ . Jahed et al. [12] presented a procedure for minimum

\* Corresponding author. Tel.: +1 540 2316051; fax: +1 540 2314574.  
E-mail addresses: [ngj@tongji.edu.cn](mailto:ngj@tongji.edu.cn) (G.J. Nie), [rbatra@vt.edu](mailto:rbatra@vt.edu) (R.C. Batra).

mass design of rotating disks with variable material properties and operating at a high temperature. Eraslan and Akis [13] obtained closed-form solutions for FG rotating solid shafts and disks by assuming that  $E$  is either an exponential or a parabolic function of  $r$ . Kordkheili and Naghdabadi [14] used a semi-analytical approach to analyze axisymmetric thermoelastic deformations of hollow and solid rotating FG disks with the thermomechanical properties given by a power-law function of  $r$ . You et al. [15] derived a closed-form solution for FG rotating disks subjected to a uniform temperature change by taking  $E$ , the thermal expansion coefficient and the mass density to vary according to power-law functions of  $r$ . Hojjati and Jafari [16] introduced two analytical methods, namely homotopy perturbation and Adomian's decomposition, to find stresses and displacements in rotating annular elastic disks with uniform and variable thicknesses and mass densities. Bayat et al. [17–20] solved the elastic and thermoelastic problems for FG rotating disks with the assumption that the material properties and disk thickness are given by power-law functions of  $r$  and the temperature field is steady. Vullo and Vivio [21,22] studied stresses and strains in variable thickness annular and solid rotating elastic disks subjected to thermal loads and having a variable density along the radius. Zenkour [23,24] investigated the stress distribution in rotating three-layer sandwich solid disks with face sheets made of different isotropic materials and a FG core.

For FGIMs, Batra [25] numerically studied axisymmetric static deformations of a Mooney–Rivlin cylinder with material parameters taken to be quadratic functions of  $r$ . Batra et al. [26–28] have found that the hoop stress in a cylinder is constant if the shear modulus is a linear function of the radius. Bilgili et al. [4–6,29,30] have analyzed shearing deformations of an inhomogeneous rubberlike slab or tube subjected to a thermal gradient across its thickness or radius.

We note that most problems for FGMs have been studied by assuming that material parameters vary either as a power-law function or an exponential function in one direction. Here we study infinitesimal deformations of a rotating disk composed of an isotropic linear thermoelastic FGIM when the shear modulus is an arbitrary smooth function of  $r$ . For a few specific variations of the shear modulus we provide exact solutions, and for a general smooth variation we solve the problem numerically by the differential quadrature method (DQM) [31]. Furthermore, we study the material tailoring problem and find either the shear modulus or the thermal expansion coefficient as a function of  $r$  to achieve a desired radial variation of stresses. For plane strain axisymmetric deformations of an FG cylinder composed of an orthotropic compressible material, Leissa and Vagins [32] assumed that all material moduli are proportional to each other and found their spatial variation so to make either the hoop stress or the shear stress uniform in the cylinder.

Qian and Batra [33] used a higher-order shear and normal deformable plate theory [34] to find the spatial variation along the axial and the thickness directions of the two constituents in a FG cantilever plate to optimize the fundamental frequency. The through-the-thickness variation of the fiber orientation angle in a fiber-reinforced laminated composite plate to optimize one of the first five lowest frequencies of a rectangular plate under different boundary conditions is given in [35], and the axial variation of the shear modulus to control the angle of twist per unit length for the torsion of a FG cylinder in [36]. Batra [37] has derived a higher-order plate theory for FGIM plates, and an exact solution for frequencies of a simply supported plate made of an incompressible material is provided in [38].

The rest of the paper is organized as follows. Section 2 gives the problem formulation, and Section 3 presents exact solutions for stresses and the radial displacement in rotating disks with the

shear modulus given by either a power-law or an exponential function of  $r$ . For a general variation of the shear modulus, the solution of the problem by the DQM is provided. The material tailoring problem is studied in Section 4, and Section 5 gives numerical examples both for the material tailoring problem, and the stress and the displacement variations in FGIM rotating disks of variable thickness under different boundary conditions. Section 6 summarizes conclusions of the work.

## 2. Problem formulation

Consider a circular disk of thickness  $h(r) > 0$  varying in the radial direction only, having inner radius,  $r_{in}$ , and outer radius,  $r_{ou}$ , and rotating at a constant angular velocity,  $\omega$ , about the centroidal axis perpendicular to the plane of the disk, as shown in Fig. 1. Assuming that  $r_{ou}/h_{max} \geq 10$  we regard the state of deformation in it to be that of plane stress, and investigate the effect of  $\omega$  on stresses induced by taking its deformations to be axisymmetric; here  $h_{max}$  equals the maximum thickness of the disk. We use cylindrical coordinate system  $(r, \theta, z)$  with the origin at the disk center and the  $z$ -axis perpendicular to the plane of the disk.

In the absence of gravitational forces, the equation of equilibrium in the radial direction is [10]

$$\frac{d}{dr}(h(r)r\sigma_{rr}) - h(r)\sigma_{\theta\theta} + h(r)\rho(r)\omega^2 r^2 = 0, \quad (1)$$

where  $\sigma_{rr}$  and  $\sigma_{\theta\theta}$  are, respectively, the radial and the hoop stresses at a point, and  $\rho(r)$  is the mass density. We solve the problem for the following three sets of boundary conditions on the inner and the outer surfaces of the disk.

Case 1: hollow disk with the inner and the outer surfaces traction free:

$$\sigma_{rr}(r_{in}) = 0.0, \quad \sigma_{rr}(r_{ou}) = 0.0. \quad (2a, b)$$

Case 2: hollow disk with the inner surface fixed and the outer surface traction free:

$$u_r(r_{in}) = 0.0, \quad \sigma_{rr}(r_{ou}) = 0.0. \quad (2c, d)$$

Case 3: solid disk with the outer surface traction free:

$$u_r(0.0) = 0.0, \quad \sigma_{rr}(r_{ou}) = 0.0, \quad (2e, f)$$

where  $u_r$  is the radial displacement of a point.

Assuming that deformations are infinitesimal, the in-plane radial and hoop strains,  $\varepsilon_{rr}$  and  $\varepsilon_{\theta\theta}$ , respectively, are related to  $u_r$  by

$$\varepsilon_{rr} = \frac{du_r}{dr}, \quad \varepsilon_{\theta\theta} = \frac{u_r}{r}. \quad (3a, b)$$

The axial strain  $\varepsilon_{zz}$  in the  $z$ -direction is generally non-zero. The compatibility equation in terms of strains is

$$\frac{d}{dr}(r\varepsilon_{\theta\theta}) - \varepsilon_{rr} = 0. \quad (4)$$

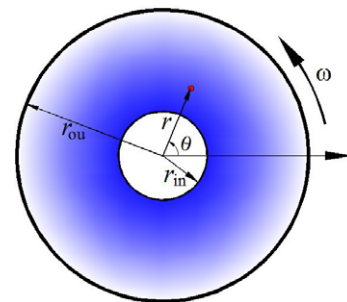


Fig. 1. Schematic sketch of the problem studied.

In linear thermoelasticity we can write strains as

$$\varepsilon_{rr} = \varepsilon_{rr}^e + \varepsilon_{rr}^T, \quad \varepsilon_{\theta\theta} = \varepsilon_{\theta\theta}^e + \varepsilon_{\theta\theta}^T, \quad \varepsilon_{zz} = \varepsilon_{zz}^e + \varepsilon_{zz}^T, \quad (5a, b, c)$$

where superscripts 'e' and 'T' denote the elastic and the thermal components of strains, respectively. The thermal strains are given by

$$\varepsilon_{rr}^T = \varepsilon_{\theta\theta}^T = \varepsilon_{zz}^T = \alpha(r)\Delta T, \quad (6)$$

where  $\Delta T$  equals the uniform temperature change measured from a stress free reference configuration, and the coefficient of thermal expansion,  $\alpha(r)$ , varies with the radius. Because only isochoric (volume preserving) deformations are admissible in an incompressible material, the elastic strain components must satisfy

$$\varepsilon_{rr}^e + \varepsilon_{\theta\theta}^e + \varepsilon_{zz}^e = 0. \quad (7)$$

The pertinent constitutive equations for an isotropic linear elastic FGIM are [40]

$$\begin{aligned} \sigma_{rr} &= -p(r) + 2G(r)\varepsilon_{rr}^e, \\ \sigma_{\theta\theta} &= -p(r) + 2G(r)\varepsilon_{\theta\theta}^e, \\ \sigma_{zz} &= -p(r) + 2G(r)\varepsilon_{zz}^e, \end{aligned} \quad (8a, b, c)$$

where  $\sigma_{zz}$  is the axial stress in the  $z$ -direction,  $p(r)$  the hydrostatic pressure not determined from the deformation field, and  $G(r) > 0$  the shear modulus. Shear stresses and shear strains vanish identically for the problem being studied.

### 3. Solutions for stresses and the radial displacement

We assume that  $r > 0$ , and solve the problem for a solid disk by taking the limit of  $r_{in}$  approaching 0.

In terms of the Airy stress function  $\varphi(r)$ , stresses  $\sigma_{rr}$  and  $\sigma_{\theta\theta}$  given by

$$\sigma_{rr} = \frac{\varphi(r)}{h(r)r}, \quad \sigma_{\theta\theta} = \frac{1}{h(r)} \frac{d\varphi(r)}{dr} + \rho(r)\omega^2 r^2, \quad (9a, b)$$

identically satisfy the equilibrium Eq. (1). Since  $\sigma_{zz} = 0$  for a state of plane stress, Eq. (8c) gives

$$\varepsilon_{zz}^e = \frac{p(r)}{2G(r)}. \quad (10)$$

Substitution from Eq. (10) into Eq. (7) gives the hydrostatic pressure

$$p(r) = -2G(r)(\varepsilon_{rr}^e + \varepsilon_{\theta\theta}^e). \quad (11)$$

Thus elastic strains in Eq. (8a, b) can be expressed in terms of stresses. In view of Eqs. (5) and (6) we get the total strains as

$$\varepsilon_{rr} = \frac{2\sigma_{rr} - \sigma_{\theta\theta}}{6G(r)} + \alpha(r)\Delta T, \quad \varepsilon_{\theta\theta} = \frac{2\sigma_{\theta\theta} - \sigma_{rr}}{6G(r)} + \alpha(r)\Delta T. \quad (12a, b)$$

Substituting for stresses from Eq. (9) into Eq. (12) and then for strains into Eq. (4), we get

$$\frac{d^2\varphi(r)}{dr^2} + f_1(r) \frac{d\varphi(r)}{dr} + f_2(r)\varphi(r) = f_3(r), \quad (13)$$

where

$$\begin{aligned} f_1(r) &= \frac{1}{r} - \frac{1}{G(r)} \frac{dG(r)}{dr} - \frac{1}{h(r)} \frac{dh(r)}{dr}, \quad f_2(r) \\ &= \frac{1}{2rG(r)} \frac{dG(r)}{dr} + \frac{1}{2rh(r)} \frac{dh(r)}{dr} - \frac{1}{r^2}, \quad f_3(r) \\ &= \omega^2 r^2 \frac{h(r)\rho(r)}{G(r)} \frac{dG(r)}{dr} - \omega^2 r^2 h(r) \frac{d\rho(r)}{dr} - \frac{7}{2} \omega^2 rh(r)\rho(r) \\ &\quad - 3\Delta TG(r)h(r) \frac{d\alpha(r)}{dr}. \end{aligned}$$

Eq. (13) is 2nd order non-homogeneous ordinary differential equation (ODE) with variable coefficients for  $\varphi(r)$ . For given  $h(r)$ ,  $G(r)$ ,  $\rho(r)$ , and  $\alpha(r)$ , we solve Eq. (13) for  $\varphi(r)$  and then find stresses from Eq. (9), strains from Eq. (12), and  $u_r$  from Eq. (3b).

We first present below exact solutions when  $G(r)$  is either a power-law or an exponential function of  $r$ . Subsequently, for an arbitrary variation of  $G(r)$  we numerically solve the problem employing the DQM.

#### 3.1. Hollow disk with power-law variation of the shear modulus, the mass density, the thermal expansion coefficient and the disk thickness

We assume that

$$\begin{aligned} G(r) &= G_{ou} \left( \frac{r}{r_{ou}} \right)^\lambda, \quad \rho(r) = \rho_{ou} \left( \frac{r}{r_{ou}} \right)^m, \quad \alpha(r) = \alpha_{ou} \left( \frac{r}{r_{ou}} \right)^t, \\ h(r) &= h_{ou} \left( \frac{r}{r_{ou}} \right)^{-n}, \quad (0 < r_{in} \leq r \leq r_{ou}), \end{aligned} \quad (14a-d)$$

where  $G_{ou}$ ,  $\rho_{ou}$ ,  $\alpha_{ou}$  and  $h_{ou}$  equal, respectively, the shear modulus, the mass density, the thermal expansion coefficient and the disk thickness at a point on the outer surface of the hollow disk, and  $\lambda$ ,  $m$ ,  $t$  and  $n$  are real numbers. For a homogeneous disk,  $\lambda$ ,  $m$ ,  $t$  and  $n$  equal zero. For a solid disk,  $\lambda$ ,  $m$  and  $t$  must be non-negative, and  $n$  must be non-positive.

Substitution for  $G(r)$ ,  $\rho(r)$ ,  $\alpha(r)$  and  $h(r)$  from Eq. (14) into Eq. (13) yields

$$\frac{d^2\varphi(r)}{dr^2} + \frac{1+n-\lambda}{r} \frac{d\varphi(r)}{dr} - \frac{2+n-\lambda}{2r^2} \varphi(r) = F(r), \quad (15)$$

where

$$\begin{aligned} F(r) &= \lambda\omega^2 h_{ou}\rho_{ou}r_{ou}^{n-m}r^{m-n+1} - m\omega^2 h_{ou}\rho_{ou}r_{ou}^{n-m}r^{m-n+1} \\ &\quad - \frac{7}{2}\omega^2 h_{ou}\rho_{ou}r_{ou}^{n-m}r^{m-n+1} - 3tG_{ou}h_{ou}\alpha_{ou}\Delta T r_{ou}^{n-t-\lambda}r^{t-n+\lambda-1}. \end{aligned} \quad (16)$$

The general solution of Eq. (15) can be written as

$$\varphi(r) = C_1 r^{s_1} + C_2 r^{s_2} + \Phi(r), \quad (17)$$

where  $C_1$  and  $C_2$  are arbitrary constants to be determined by using boundary conditions in Eq. (2);  $s_1$  and  $s_2$  are real roots of the quadratic equation

$$s^2 + (n-\lambda)s + \frac{1}{2}(\lambda-n-2) = 0, \quad (18)$$

and

$$\Phi(r) = -\frac{4h_{ou}(\chi_1 - \chi_2)r_{ou}^{n-m-t-\lambda}r^{1-n}}{\chi_3\chi_4}, \quad (19)$$

is the particular solution of Eq. (15), where

$$\begin{aligned} \chi_1 &= \rho_{ou}\omega^2 r_{ou}^{t+\lambda} r^{m+2} (2m-2\lambda+7)(2t^2-n(2t+3)+2t(\lambda+2)+3\lambda), \\ \chi_2 &= 6tG_{ou}\alpha_{ou}\Delta T r_{ou}^m r^{t+\lambda} (2m^2-2m(n+\lambda-6)+n(2\lambda-7)-5\lambda+16), \\ \chi_3 &= 4m(n+\lambda-6)+n(14-4\lambda)+10\lambda-4m^2-32, \\ \chi_4 &= n(4t+6)-2(2t^2+3\lambda+2t(\lambda+2)). \end{aligned}$$

Knowing the stress function  $\varphi(r)$ , we get following expressions for stresses and the hydrostatic pressure:

$$\begin{aligned} \sigma_{rr} &= \frac{C_1 r^{s_1+n-1}}{h_{ou}r_{ou}^n} + \frac{C_2 r^{s_2+n-1}}{h_{ou}r_{ou}^n} + \frac{\Phi(r)r^{n-1}}{h_{ou}r_{ou}^n}, \\ \sigma_{\theta\theta} &= \frac{C_1 s_1 r^{s_1+n-1}}{h_{ou}r_{ou}^n} + \frac{C_2 s_2 r^{s_2+n-1}}{h_{ou}r_{ou}^n} + \frac{r^n}{h_{ou}r_{ou}^n} \frac{d\Phi(r)}{dr} + \frac{\rho_{ou}\omega^2 r^{m+2}}{r_{ou}^m}, \\ p(r) &= -\frac{C_1(s_1+1)r^{s_1+n-1}}{3h_{ou}r_{ou}^n} - \frac{C_2(s_2+1)r^{s_2+n-1}}{3h_{ou}r_{ou}^n} \\ &\quad - \frac{r^n}{3h_{ou}r_{ou}^n} \frac{d\Phi(r)}{dr} - \frac{r^{n-1}\Phi(r)}{3h_{ou}r_{ou}^n} - \frac{\rho_{ou}\omega^2 r^{m+2}}{3r_{ou}^m}. \end{aligned} \quad (20a, b, c)$$

Substitution for stresses from Eq. (20) into Eq. (12b) and the result into Eq. (3b) gives

$$u_r = \frac{r^{n-\lambda+1}}{3h_{ou}G_{ou}r_{ou}^{n-\lambda}} \frac{d\Phi(r)}{dr} - \frac{r^{n-\lambda}\Phi(r)}{6h_{ou}G_{ou}r_{ou}^{n-\lambda}} + \frac{\rho_{ou}\omega^2 r^{m-\lambda+3}}{3G_{ou}r_{ou}^{m-\lambda}} + \alpha_{ou} \frac{r^{t+1}}{r_{ou}^t} \Delta T + F(r), \tag{21a}$$

where

$$F(r) = \frac{C_1(2s_1 - 1)r^{s_1+n-\lambda} + C_2(2s_2 - 1)r^{s_2+n-\lambda}}{6h_{ou}G_{ou}r_{ou}^{n-\lambda}}. \tag{21b}$$

Constants  $C_1$  and  $C_2$  in Eqs. (20) and (21) are determined from boundary conditions (2). We thus have the exact solution for stresses and the radial displacement in a uniformly heated FGIM rotating disk with the shear modulus, the mass density, the thermal expansion coefficient, and the disk thickness varying as power-law functions of the radius.

3.2. Hollow disk with exponential variation of the shear modulus but constant mass density, thermal expansion coefficient and disk thickness

Suppose that  $G(r)$  is given by

$$G(r) = G_0 \exp(\beta r/r_{ou}), \quad (\beta \neq 0), \tag{22}$$

where  $G_0$  equals the shear modulus at a point of the disk, and  $\beta$  is a constant. The disk has a uniform thickness  $h_0$  and mass density  $\rho_0$ . Substitution for  $G(r)$  from Eq. (22) into Eq. (13) gives

$$\frac{d^2\varphi(r)}{dr^2} + \left(\frac{1}{r} - \frac{\beta}{r_{ou}}\right) \frac{d\varphi(r)}{dr} + \left(\frac{\beta}{2r_{ou}r} - \frac{1}{r^2}\right) \varphi(r) = g(r), \tag{23}$$

where  $g(r) = \omega^2\beta h_0\rho_0 r^2/r_{ou} - \frac{7}{2}\omega^2 h_0\rho_0 r$ . Note from Eq. (23) that there are no thermal stresses in a uniformly heated rotating disk with constant thermal expansion coefficient.

The general solution of the homogeneous equation associated with Eq. (23) is

$$\varphi^g(r) = A_1 r U(a_1, 3, a_2) + A_2 r L_{-a_1}^2(a_2), \tag{24}$$

where constants  $A_1$  and  $A_2$  are determined by boundary conditions (2),  $U(a, b, z)$  is the confluent hypergeometric function

$$U(a, b, z) = (1/\Gamma(a)) \int_0^\infty e^{-zt} t^{a-1} (1+t)^{b-a-1} dt,$$

$L_n^a(x)$  is the generalized Laguerre polynomial, and  $a_1 = \frac{1}{2}$ ,  $a_2 = \frac{\beta r}{r_{ou}}$ .

We employ the power series method to derive the particular solution of Eq. (23). Considering the form of the non-homogeneous term  $g(r)$ , the particular solution of Eq. (23) is assumed to be

$$\varphi^p(r) = \sum_{i=0}^3 b_i r^i, \tag{25}$$

where coefficients  $b_i$ ,  $i = 0, 1, 2, 3$ , are to be determined. Substituting from Eq. (25) into Eq. (23) and equating coefficients of like powers of  $r$  on both sides of the resulting equation, we get

$$\varphi^p(r) = \frac{\omega^2 h_0 \rho_0 (6r_{ou}^2 r + \beta r_{ou} r^2 - 2\beta^2 r^3)}{5\beta^2}. \tag{26}$$

Thus the solution of Eq. (23) is

$$\varphi(r) = \varphi^g(r) + \varphi^p(r), \tag{27}$$

and we can find the corresponding stresses and the radial displacement.

3.3. Arbitrary variations of the shear modulus, mass density, thermal expansion coefficient and disk thickness

For an arbitrary smooth function  $G(r)$  we are unable to find a closed-form solution of Eq. (13). Here we use the DQM [31] which postulates that for a continuous function  $f(\xi)$  defined for  $\xi \in [0, 1]$  the value of the  $n$ th derivative of the function at an arbitrary point  $\xi_i$  in  $[0, 1]$  can be approximated by the linear sum of weighted values of  $f(\xi)$  at  $N$  discrete points in  $[0, 1]$ . That is,

$$\frac{d^n f(\xi_i)}{d\xi^n} = \sum_{j=1}^N w_{ij}^{(n)} f(\xi_j), \quad (n = 1, 2, \dots, N - 1), \tag{28}$$

where  $N$  is the total number of sampling points in  $[0, 1]$ ,  $w_{ij}^{(n)}$  are the weights for the  $n$ th order derivative. Explicit expressions for  $w_{ij}^{(n)}$ , given in Shu [31], are omitted here. Three ways to choose sampling point distributions are to place them uniformly in the domain, use the Chebyshev–Gauss–Lobatto grid, and a grid with coordinates that are roots of the Chebyshev polynomial [31].

We first write Eq. (13) in terms of the following non-dimensional variables:

$$\begin{aligned} R &= \frac{r}{r_{ou}}, \quad H = \frac{h}{h_0}, \quad \bar{\rho} = \frac{\rho}{\rho_0}, \quad \bar{\varphi} = \frac{\varphi}{h_0 \rho_0 \omega^2 r_{ou}^3}, \\ \bar{G} &= \frac{G}{\rho_0 \omega^2 r_{ou}^2}, \quad \bar{U}_r = \frac{u_r}{r_{ou}}, \quad \bar{\sigma}_{rr} = \frac{\sigma_{rr}}{\rho_0 \omega^2 r_{ou}^2}, \\ \bar{\sigma}_{\theta\theta} &= \frac{\sigma_{\theta\theta}}{\rho_0 \omega^2 r_{ou}^2}, \quad \bar{p} = \frac{p}{\rho_0 \omega^2 r_{ou}^2}, \end{aligned} \tag{29}$$

where  $h_0$  and  $\rho_0$  are values of the thickness and the mass density at a point of the disk. Setting

$$f_G(r) = \frac{1}{G(r)} \frac{dG(r)}{dr}, \tag{30}$$

we get  $f_G(r) = f_G(R)/r_{ou}$  and the non-dimensional form of Eq. (13) is

$$\frac{d^2 \bar{\varphi}(R)}{dR^2} + \delta_1 \frac{d\bar{\varphi}(R)}{dR} + \delta_2 \bar{\varphi}(R) = \delta_3, \tag{31}$$

where

$$\begin{aligned} \delta_1 &= \frac{1}{R} - f_G(R) - \frac{1}{H} \frac{dH}{dR}, \quad \delta_2 = \frac{f_G(R)}{2R} - \frac{1}{R^2} + \frac{1}{2HR} \frac{dH}{dR}, \\ \delta_3 &= H\bar{\rho} f_G(R) R^2 - \frac{7}{2} H\bar{\rho} R - H \frac{d\bar{\rho}}{dR} R^2 - 3\bar{G}(R) \Delta TH \frac{d\alpha}{dR}. \end{aligned}$$

Applying the DQM to Eq. (31) with sampling points  $R_i (i = 1, 2, \dots, N)$  with  $R_1 = r_{in}/r_{ou}$  and  $R_N = 1$ , we get the following set of  $N - 2$  simultaneous algebraic equations for  $i = 2, \dots, N - 1$ :

$$\sum_{j=1}^N w_{ij}^{(2)} \bar{\varphi}(R_j) + \gamma_1 \sum_{j=1}^N w_{ij}^{(1)} \bar{\varphi}(R_j) + \gamma_2 \bar{\varphi}(R_i) = \gamma_3, \tag{32}$$

where

$$\begin{aligned} \gamma_1 &= \frac{1}{R_i} - f_G(R_i) - \frac{1}{H(R_i)} \sum_{j=1}^N w_{ij}^{(1)} H(R_j), \\ \gamma_2 &= \frac{f_G(R_i)}{2R_i} - \frac{1}{R_i^2} + \frac{1}{2H(R_i)R_i} \sum_{j=1}^N w_{ij}^{(1)} H(R_j), \\ \gamma_3 &= H(R_i) \bar{\rho}(R_i) f_G(R_i) R_i^2 - \frac{7}{2} H(R_i) \bar{\rho}(R_i) R_i - H(R_i) R_i^2 \sum_{j=1}^N w_{ij}^{(1)} \bar{\rho}(R_j) \\ &\quad - 3\bar{G}(R_i) \Delta TH(R_i) \sum_{j=1}^N w_{ij}^{(1)} \alpha(R_j). \end{aligned}$$

Equations corresponding to  $i = 1$  and  $N$  are obtained by satisfying the discrete form of the two boundary conditions. The solution of these  $N$  algebraic equations provides values of the stress function

at the  $N$  discrete points. For  $R_i \neq 0$ , stresses and the hydrostatic pressure at the discrete points are given by

$$\begin{aligned}\bar{\sigma}_{rr}(R_i) &= \frac{\bar{\varphi}(R_i)}{R_i}, \quad \bar{\sigma}_{\theta\theta}(R_i) = \sum_{j=1}^N w_{ij}^{(1)} \bar{\varphi}(R_j) + R_i^2, \\ \bar{p}(R_i) &= -\frac{1}{3} \sum_{j=1}^N w_{ij}^{(1)} \bar{\varphi}(R_j) - \frac{\bar{\varphi}(R_i)}{3R_i} - \frac{R_i^2}{3}.\end{aligned}\quad (33a, b, c)$$

For  $R_i \neq 0$ , the radial displacement at  $R_i$  ( $i = 1, 2, \dots, N$ ) is obtained by substituting for stresses into Eq. (12b) and the result into Eq. (3b):

$$U_r(R_i) = \frac{R_i}{6G(R_i)} \left( 2 \sum_{j=1}^N w_{ij}^{(1)} \bar{\varphi}(R_j) + 2R_i^2 - \frac{\bar{\varphi}(R_i)}{R_i} \right) + \Delta T \alpha(R_i) R_i. \quad (34)$$

For a solid disk, stresses and the displacement at the center  $R_1 = 0$  of the disk obtained by the limiting process are given by

$$\bar{\sigma}_{rr}(R_1) = \bar{\sigma}_{\theta\theta}(R_1) = \sum_{j=1}^N w_{1j}^{(1)} \bar{\varphi}(R_j) + R_1^2, \quad U_r(R_1) = 0. \quad (35, 36)$$

#### 4. Material tailoring to achieve desirable stress states

We now analyze the problem of finding the function  $G(r)$  when the hoop and the radial stresses satisfy the relation

$$k\sigma_{rr} + \sigma_{\theta\theta} = D_0, \quad (37)$$

where  $k$  is a known constant, and the constant  $D_0$  is consistent with the specified boundary conditions. For  $k = 0$ , Eq. (37) implies that the hoop stress is constant, and for  $k = -1$  the in-plane shear stress is constant.

Substituting for the mass density from Eq. (14b) and the disk thickness from Eq. (14d) into Eq. (9) and the result into Eq. (37), we get for  $m \neq -2$  the following expressions for the stress function in view of the boundary conditions (2a, b):

$$\varphi(r) = \frac{\rho_{ou} h_{ou} \omega^2 r^{n-m} (g_1 r^{-k} + g_2 r^{m-n+3} + g_3 r^{1-n})}{(m-n+k+3)(r_{in}^{k+1} r_{ou}^n - r_{in}^n r_{ou}^{k+1})},$$

when  $k-n+1 \neq 0$ , (38a)

$$\varphi(r) = \frac{\rho_{ou} h_{ou} \omega^2 r^{1-m} ((r_{in}^{m+2} - r_{ou}^{m+2}) \ln r + \ln(r_{ou}/r_{in}) r^{m+2} + g_4)}{(m+2) \ln(r_{in}/r_{ou})},$$

when  $k = 0, n = 1$ , (38b)

$$\varphi(r) = \frac{\rho_{ou} h_{ou} \omega^2 r^{-m} ((r_{in}^{m+2} - r_{ou}^{m+2}) \ln r + \ln(r_{ou}/r_{in}) r^{m+2} + g_4)}{(m+2) \ln(r_{in}/r_{ou})},$$

when  $k = -1, n = 0$ , (38c)

where  $g_1 = r_{in}^{k+1} r_{ou}^{k+1} (r_{ou}^{m+2} - r_{in}^{m+2})$ ,  $g_2 = r_{in}^n r_{ou}^{k+1} - r_{in}^{k+1} r_{ou}^n$ ,  $g_3 = r_{in}^{m+k+3} r_{ou}^n - r_{in}^n r_{ou}^{m+k+3}$ ,  $g_4 = r_{ou}^{m+2} \ln r_{in} - r_{in}^{m+2} \ln r_{ou}$ . For  $m = -2$ , the stress function equals zero and the disk must be hollow with the inner and the outer surfaces traction free. In this case, the radial stress identically vanishes, the hoop stress equals  $\rho_{ou} (r_{ou} \omega_{ou})^2$ . Henceforth, we assume that  $m \neq -2$ . Knowing  $\varphi(r)$ ,  $\rho(r)$  and  $h(r)$ , we obtain the desired stress distribution (37) by tailoring the variation in the radial direction of the shear modulus or the thermal expansion coefficient.

Case 1: For constant thermal expansion coefficient  $\alpha(r) = \alpha_0$ , the function  $G(r)$  to attain the stress distribution (37) is given by

$$G(r) = G_{in} \exp \left[ \int_{r_{in}}^r f(x) dx \right], \quad (39)$$

where  $G_{in}$  equals the value of  $G$  at a point on the inner surface of the disk, and

$$\begin{aligned}f(x) &= \frac{f_1(x)}{f_2(x)}, \quad f_2(x) = \frac{d\varphi(x)}{dx} - \frac{\varphi(x)}{2x} + \omega^2 x^2 h(x) \rho(x), \\ f_1(x) &= \frac{d^2 \varphi(x)}{dx^2} + \left( \frac{1}{x} - \frac{1}{h(x)} \frac{dh(x)}{dx} \right) \frac{d\varphi(x)}{dx} + \left( \frac{1}{2xh(x)} \frac{dh(x)}{dx} - \frac{1}{x^2} \right) \varphi(x) \\ &\quad + \omega^2 x^2 h(x) \frac{d\rho(x)}{dx} + \frac{7}{2} \omega^2 x h(x) \rho(x).\end{aligned}$$

It is difficult to evaluate in closed-form the integral in Eq. (39); however, one can evaluate it numerically.

For a solid disk of constant mass density  $\rho_0$  and thermal expansion coefficient  $\alpha_0$  and uniform thickness  $h_0$ , the variation of the shear modulus for the hoop stress to be constant in the disk is given by

$$G(r) = G_{in} \left( 1 + \frac{r^2}{r_{ou}^2} \right)^{\frac{5}{2}}, \quad (40)$$

where  $G_{in}$  equals the shear modulus at the disk center. The corresponding stresses, the hydrostatic pressure and the radial displacement are:

$$\begin{aligned}\sigma_{rr} &= \frac{\rho_0 \omega^2}{3} (r_{ou}^2 - r^2), \quad \sigma_{\theta\theta} = \frac{\rho_0 \omega^2 r_{ou}^2}{3}, \\ p(r) &= \frac{\rho_0 \omega^2}{9} (r^2 - 2r_{ou}^2).\end{aligned}\quad (41a, b, c)$$

$$u_r = \frac{\rho_0 \omega^2 r_{ou}^5}{18 G_{in}} r (r^2 + r_{ou}^2)^{-\frac{3}{2}} + \alpha_0 \Delta T r. \quad (42)$$

Case 2: For constant shear modulus  $G(r) = G_0$ , the thermal expansion coefficient to attain the stress distribution (37) is given by

$$\alpha(r) = \alpha_{in} + \int_{r_{in}}^r \frac{y(x)}{3G_0 \Delta T h(x)} dx, \quad (43)$$

where  $\alpha_{in}$  is the value of  $\alpha$  at the point  $r = r_{in}$  within the disk, and  $y(x) = y_1(x) + y_2(x)$ ,

$$\begin{aligned}y_1(x) &= -\omega^2 x^2 h(x) \frac{d\rho(x)}{dx} - \frac{7}{2} \omega^2 x h(x) \rho(x), \\ y_2(x) &= -\frac{d^2 \varphi(x)}{dx^2} - \left( \frac{1}{x} - \frac{1}{h(x)} \frac{dh(x)}{dx} \right) \frac{d\varphi(x)}{dx} - \left( \frac{1}{2xh(x)} \frac{dh(x)}{dx} - \frac{1}{x^2} \right) \varphi(x).\end{aligned}$$

From Eq. (43), it is noticed that the desired stress field can be achieved by adjusting the variation of the thermal expansion coefficient with the radial coordinate even if the shear modulus of FGIMs is constant.

For an annular disk of constant shear modulus  $G_0$ , mass density  $\rho_0$ , and thickness  $h_0$  under the boundary condition in Eq. (2a, b), the variation of the thermal expansion coefficient for the hoop stress to be constant in the disk is given by

$$\alpha(r) = \alpha_{ou} + \frac{\rho_0 \omega^2 (r_{ou} - r) (5r^2 + 5r_{ou}r + 4r_{in}(r_{in} + r_{ou}))}{36G_0 \Delta T r}, \quad (44)$$

where  $\alpha_{ou}$  equals the thermal expansion coefficient at the outer surface of the disk. The corresponding stresses, the hydrostatic pressure and the displacement are

$$\begin{aligned}\sigma_{rr} &= -\frac{\rho_0 \omega^2}{3r} (r - r_{in})(r - r_{ou})(r + r_{in} + r_{ou}), \\ \sigma_{\theta\theta} &= \frac{\rho_0 \omega^2 (r_{in}^2 + r_{in} r_{ou} + r_{ou}^2)}{3}, \\ p(r) &= \frac{\rho_0 \omega^2}{9r} (r^3 - 2(r_{in}^2 + r_{in} r_{ou} + r_{ou}^2)r + r_{in} r_{ou} (r_{in} + r_{ou})),\end{aligned}\quad (45a, b, c)$$

$$u_r = \frac{\rho_0 \omega^2}{36G_0} (-3r^3 + (7r_{ou}^2 - 2r_{in}^2 - 2r_{in} r_{ou})r + 6r_{in} r_{ou} (r_{in} + r_{ou})) + \alpha_{ou} \Delta T r. \quad (46)$$

For a solid disk of constant shear modulus  $G_0$ , mass density  $\rho_0$ , and thickness  $h_0$ , the variation of the thermal expansion coefficient for the hoop stress to be constant in the disk is given by

$$\alpha(r) = \alpha_0 - \frac{5\rho_0\omega^2 r^2}{36G_0\Delta T}, \tag{47}$$

where  $\alpha_0$  equals the thermal expansion coefficient at the disk center. The corresponding stresses are the same as those in Eq. (41) and the displacement is

$$u_r = \frac{\rho_0\omega^2}{36G_0}(-3r^3 + 2r_{ou}^2 r) + \alpha_0\Delta T r. \tag{48}$$

**5. Numerical examples**

5.1. Stress analysis

**Example 1.** Hollow disk with power-law variations of  $G(r)$ ,  $\rho(r)$ ,  $\alpha(r)$  and  $h(r)$ .

For a hollow disk with  $r_{in}/r_{ou} = 0.2$  rotating at a constant angular velocity, and  $G(r)$ ,  $\rho(r)$ ,  $\alpha(r)$  and  $h(r)$  given by Eqs. (14a–d), we have plotted in Figs. 2–8 the non-dimensional stresses  $\bar{\sigma}_{rr} = \sigma_{rr}/(\rho_{ou}\omega^2 r_{ou}^2)$ ,  $\bar{\sigma}_{\theta\theta} = \sigma_{\theta\theta}/(\rho_{ou}\omega^2 r_{ou}^2)$  for  $\lambda = -1, 0, 1$ ,  $m = -1, 0, 1$ ,  $n = -1, 0, 1$ , and thermal stresses for  $t = -1, 0, 1$ , and  $\Delta T = \rho_{ou}\omega^2 r_{ou}^2 / (G_{ou}\alpha_{ou})$  with disk's inner surface either fixed or traction free. Results in Figs. 2–8 for  $\lambda = m = t = n = 0$  are for a homogeneous disk.

Stresses at a point depend continuously upon the variables  $m$ ,  $n$  and  $\lambda$  since they do not exhibit any discontinuities for the three discrete values assigned to  $m$ ,  $n$  and  $\lambda$ . In Fig. 2a and b, the qualitative distribution of  $\bar{\sigma}_{rr}$  is same for the three values of  $\lambda$ , but that for  $\bar{\sigma}_{\theta\theta}$  is quite different for the three values of  $\lambda$ . For  $\lambda = 1$ ,  $\bar{\sigma}_{\theta\theta}$  is nearly constant throughout the disk. Recall that for a hollow cylinder loaded by uniform pressures on the inner and the outer surfaces, the hoop stress is constant when  $G(r)$  is a linear function of  $r$ . For the disk the non-uniform distribution of the centrifugal force requires that the hoop stress vary in the radial direction. The hoop stress at the non-dimensional radius of  $0.45 = (0.2)^{1/2} = (r_{in}r_{ou})^{1/2}$

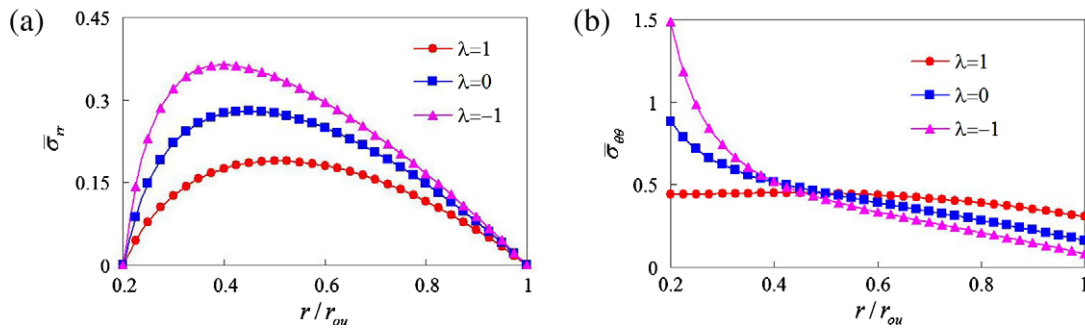


**Fig. 2.** For free–free hollow rotating disk of constant thickness, thermal expansion coefficient and mass density, variations with the radius of (a) the radial stress and (b) the hoop stress for three values of the gradation index  $\lambda$  in the expression for the shear modulus.

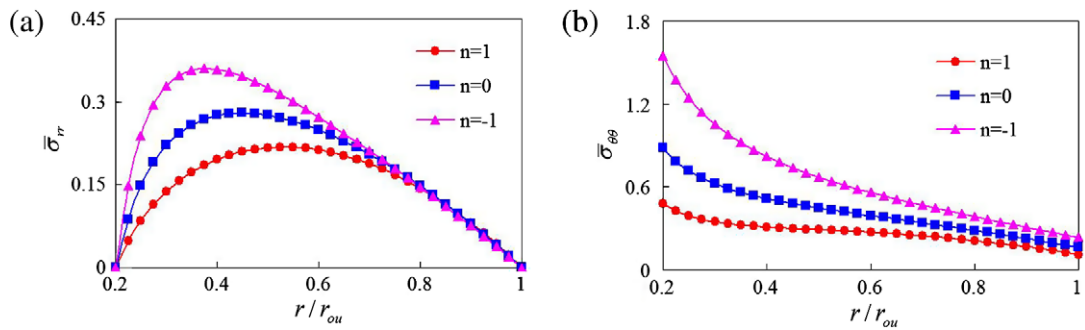


**Fig. 3.** For free–free hollow rotating disk of constant mass density, thermal expansion coefficient and shear modulus, variations with the radius of (a) the radial stress and (b) the hoop stress for three values of the gradation index  $n$  in the expression for the disk thickness.

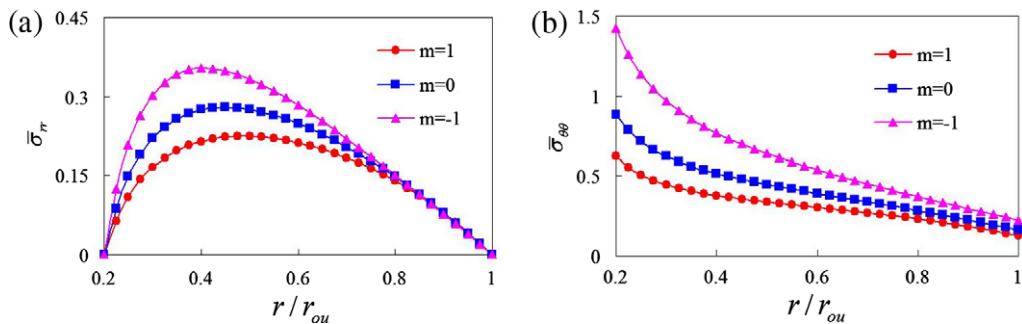


**Fig. 4.** For free–free hollow rotating disk of constant thickness, thermal expansion coefficient and shear modulus, variations with the radius of (a) the radial stress and (b) the hoop stress for three values of the gradation index  $m$  in the expression for the mass density.

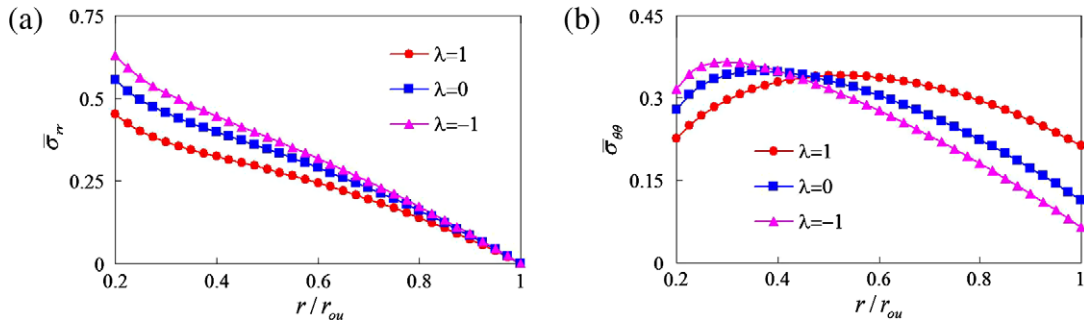


Fig. 5. For fixed–free hollow rotating disk of constant thickness, thermal expansion coefficient and mass density, variations with the radius of (a) the radial stress and (b) the hoop stress for three values of the gradation index  $\lambda$  in the expression for the shear modulus.

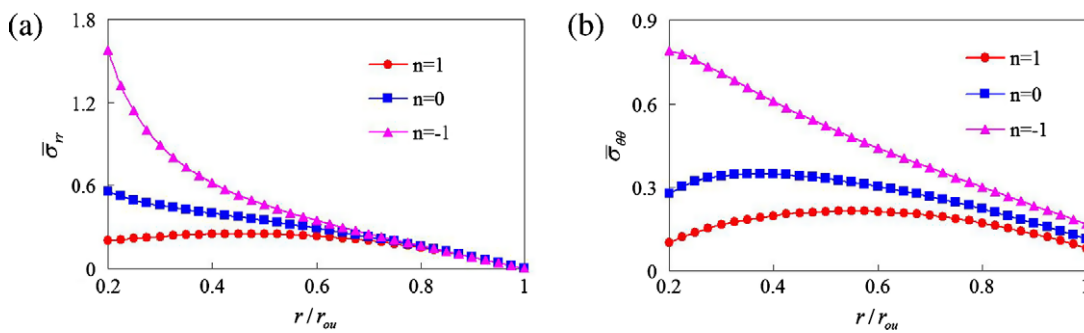


Fig. 6. For fixed–free hollow rotating disk of constant mass density, thermal expansion coefficient and shear modulus, variations with the radius of (a) the radial stress and (b) the hoop stress for three values of the gradation index  $n$  in the expression for the disk thickness.

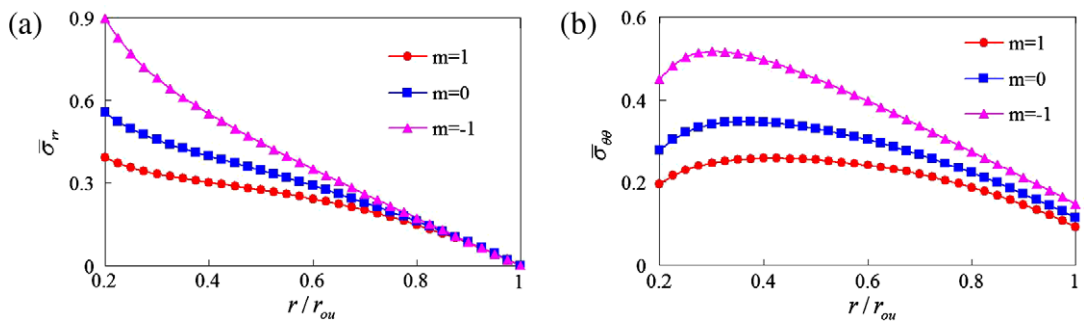


Fig. 7. For fixed–free hollow rotating disk of constant thickness, thermal expansion coefficient and shear modulus, variations with the radius of (a) the radial stress and (b) the hoop stress for three values of the gradation index  $m$  in the expression for the mass density.

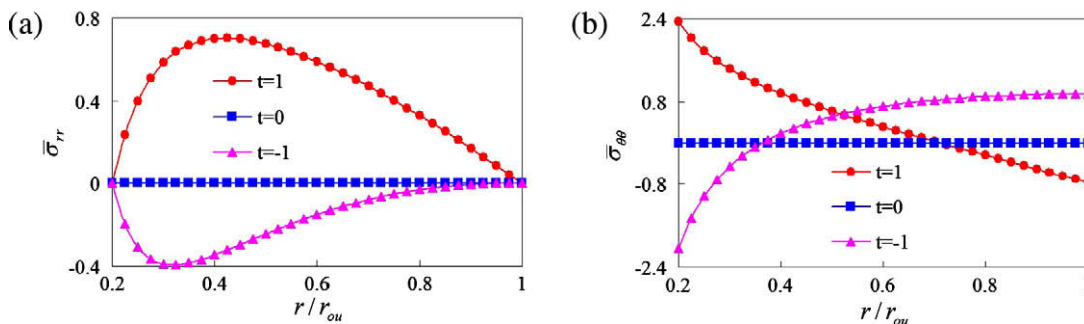
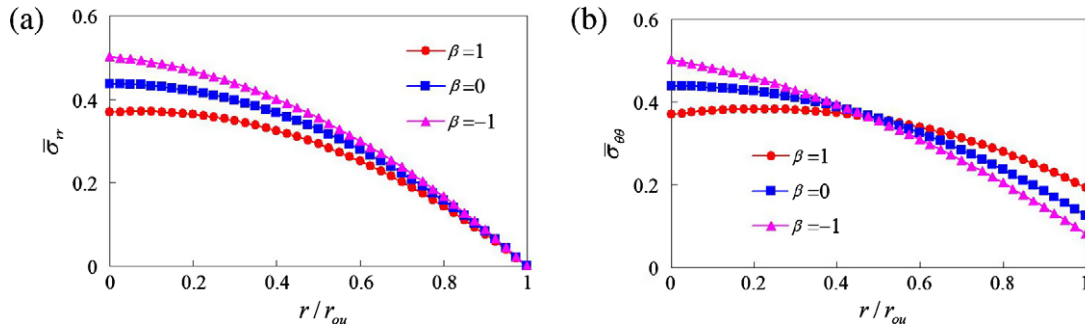


Fig. 8. For free–free hollow rotating disk of constant thickness, mass density and shear modulus, variations with the radius of (a) the radial stress and (b) the hoop stress for three values of the gradation index  $t$  in the expression for the thermal expansion coefficient.



**Fig. 9.** For a rotating solid disk with uniform thickness, mass density and thermal expansion coefficient, variations with the radius of (a) the radial stress and (b) the hoop stress for three values of the gradation index  $\beta$  in the expression for the shear modulus.

is nearly the same for the three values of  $\lambda$ ; a similar result was obtained in [27] for a hollow circular FG cylinder.

When  $h(r)$  is a power-law function of  $r$ , stresses exhibited in Fig. 3a and b reveal that with an increase in the value of  $n$  from  $-1$  to  $1$  the point where the peak radial stress occurs moves away from the inner surface of the hollow disk, and the maximum value of  $\bar{\sigma}_{\theta\theta}$  at a point on the inner surface decreases. The effect of varying the mass density in the radial direction is qualitatively similar to that of changing the disk thickness; cf. Fig. 4a and b.

We have displayed in Fig. 5a and b stresses vs. the radius for a hollow disk with the inner surface fixed, the outer surface traction free and  $G(r)$  a power-law function of  $r$ . The stress distributions are

qualitatively similar for  $\lambda = -1, 0, 1$  with the maximum radial stress occurring at a point on the inner fixed surface and the maximum hoop stress at a point inside the disk. The hoop stress at  $r = 0.45r_{ou}$  is nearly the same for the three values of  $\lambda$ . The comparison of stress distributions in Figs. 2 and 5 reveals that fixing the inner surface of the disk considerably reduces the peak hoop stress but increases the maximum radial stress. The maximum radial stress at a point on the inner surface of the fixed-free disk in Fig. 6a for  $n = -1$  is nearly 7.8 times of that for  $n = 1$  and the two values of the maximum hoop stress in Fig. 6b differ by a factor of about 3.5. Note that for  $n = -1$  and  $1$ , the disk thickness is minimum and maximum, respectively, at its inner surface. From plots of stresses in Fig. 7 we conclude that changes in the mass density have less dramatic effect on the peak radial and hoop stresses as compared to those in the disk thickness. For example, the ratio of the peak hoop stresses for  $m = 1$  and  $-1$  is about 2. For a fixed-free hollow disk, the maximum radial stress is greater than the maximum hoop stress but the reverse holds for a free-free hollow disk. Both for the free-free and the fixed-free disks, the maximum stresses for  $\lambda = -1, m = -1$  or  $n = -1$  are more than those for a homogeneous disk. Thus an improper gradation of material or geometric parameters may enhance peak stresses rather than reduce them.

**Table 1**  
Comparison of stresses in the solid disk from two methods.

	R	DQM solution			Exact
		N = 7	N = 11	N = 21	
Hoop stress	0.0	0.369432	0.369432	0.369432	0.369432
	0.5	0.359161	0.359161	0.359161	0.359161
	1.0	0.193692	0.193692	0.193692	0.193692
Radial stress	0.5	0.293146	0.293146	0.293146	0.293146

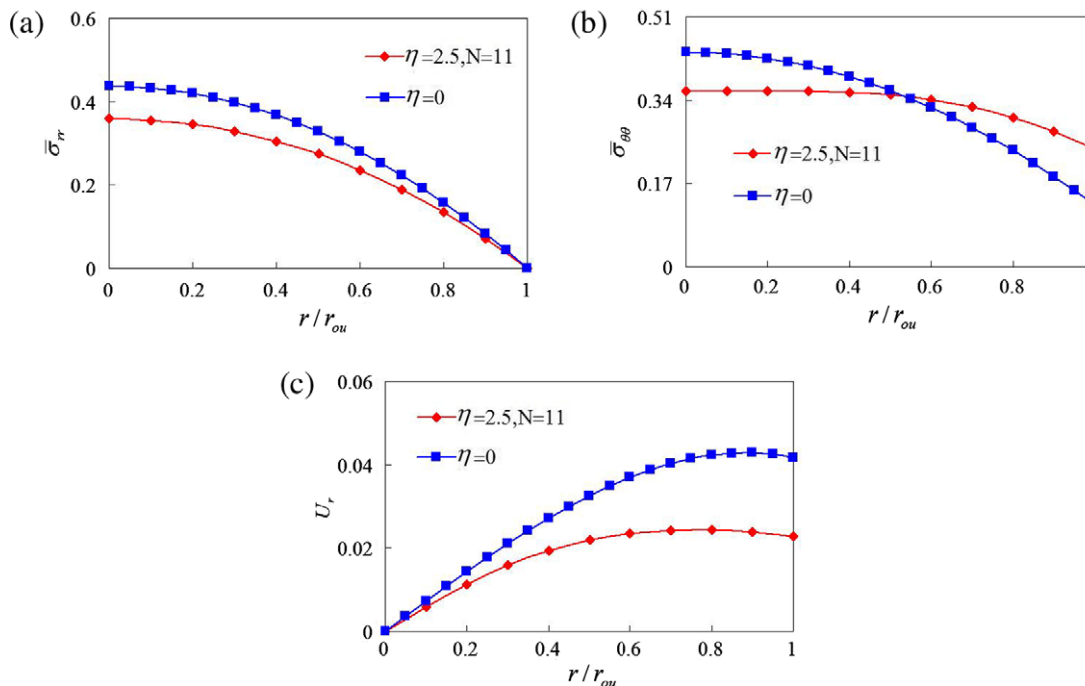


**Fig. 10.** For a rotating solid disk with uniform thickness, mass density and thermal expansion coefficient, variations of (a) the radial stress, (b) the hoop stress, and (c) the radial displacement with the radius for different values of the gradation parameter  $\eta$  in Eq. (49) for the shear modulus.

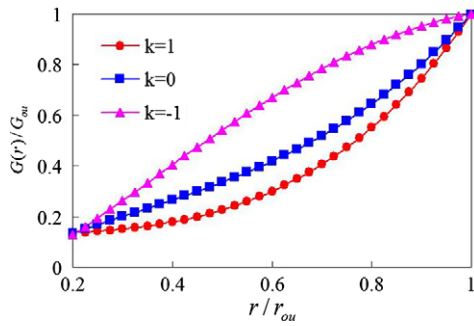


**Fig. 11.** For a free-free hollow rotating disk with uniform thickness, thermal expansion coefficient and density, the required variation of the shear modulus along the radial direction for achieving three different states of stress.

As expected, results depicted in Fig. 8 reveal that no thermal stresses are induced in the uniformly heated homogeneous disk with the inner and the outer surfaces traction free. However, when the coefficient of thermal expansion varies in the radial direction, the radial stress is tensile when the gradation index  $t > 0$  and is compressive for  $t < 0$ . The maximum magnitude of the hoop stress occurs at a point on the inner surface of the disk and signs of the hoop stresses at points on the inner and the outer surfaces of the disk are opposite of each other. These results agree qualitatively with those reported in [39].

**Example 2.** Solid disk with exponential variation of the shear modulus but constant mass density, thermal expansion coefficient and disk thickness

The non-dimensional radial stress  $\bar{\sigma}_{rr}$  and hoop stress  $\bar{\sigma}_{\theta\theta}$  for a solid disk with  $\beta = -1, 0, 1$  in Eq. (22) are calculated from the analytical expressions given in Section 3.2, and are exhibited in Fig. 9; results for  $\beta = 0$  are for a homogeneous disk. These results evince that the exponential variation of the shear modulus does not change the stress distribution dramatically when  $\beta$  is varied from  $-1$  to  $1$ .

For  $\beta = 1$  stresses in the solid disk are also calculated with the DQM using uniform spacing of sampling points with point 1 located at the disk center, and are compared in Table 1 with those obtained from the analytical solution. At point 1, boundary condition (36) replaces Eq. (32) and  $U(R)$  is not singular at  $R = 0$ . It is clear that, at least for this problem, results from the DQM agree well with those from the exact solution and the number of sampling points has very little effect on the results.

**Example 3.** Solid disk of constant mass density, thermal expansion coefficient and thickness but the shear modulus a function of the radius.

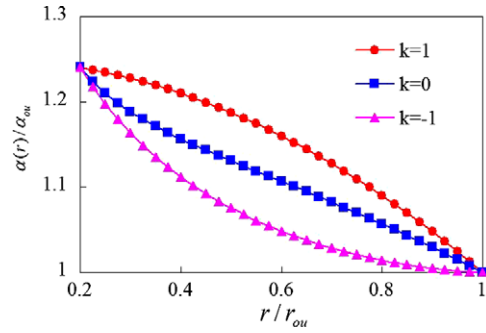


**Fig. 13.** For a free-free hollow rotating disk with uniform thickness, shear modulus and density, the required variation of the thermal expansion coefficient along the radial direction for achieving three different states of stress.

For a solid disk of uniform mass density, thermal expansion coefficient and thickness, and the shear modulus given by

$$G(r) = G_0(1 + \eta r^2/r_{ou}^2), \tag{49}$$

we have used the DQM to analyze the problem. The variation in the radial direction of  $\bar{\sigma}_{rr}$ ,  $\bar{\sigma}_{\theta\theta}$  and the non-dimensional radial displacement  $U_r$  for two values of  $\eta$  are exhibited in Fig. 10; results for  $\eta = 0$  are for a homogeneous disk; and those for  $\eta = 2.5$  have been computed by taking eleven uniformly spaced points in  $[0, 1]$ . These results evince that the radial and the hoop stresses at the disk center are reduced by 20% when  $\eta$  in Eq. (49) is changed from 0 to 2.5. For  $\eta = 2.5$ , the hoop stress is nearly uniform over the inner half of the disk implying that the material strength is fully utilized. The radial displacement of a point on the outer surface of the FG disk is nearly one-half of that for the identical homogeneous disk.

5.2. Material tailoring

**Example 4.** Material tailoring for a free-free hollow disk of variable mass density and thickness.

For a free-free hollow disk with  $r_{in}/r_{ou} = 0.2$  rotating at a constant angular velocity with either constant thickness and mass density or the mass density and the disk thickness varying linearly in the radial direction, we have plotted in Figs. 11–13 the required radial variation of the shear modulus or the thermal expansion coefficient to have either the hoop stress or the sum of the radial and the hoop stresses or the in-plane shear stress constant. It is clear that for each case, the shear modulus and thermal expansion coefficient vary smoothly with the radius. Whereas the shear modulus is an increasing function of the radius, the thermal expansion coefficient is a decreasing function of the radius to achieve the same desirable stress distribution in the disk. The ratio of the shear

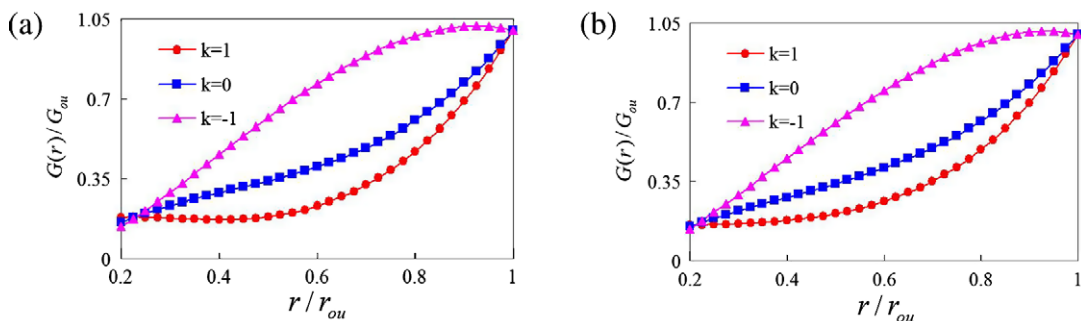


**Fig. 12.** For a free-free hollow rotating disk with constant thermal expansion coefficient, the variation of the shear modulus along the radial direction for achieving three different states of stress with (a) constant mass density but linearly varying thickness ( $m = 0$  and  $n = 1$ ) and (b) linearly varying mass density but constant thickness ( $m = 1$  and  $n = 0$ ).

modulus at points on the outer and the inner surfaces is about 7.5 and that of the thermal expansion coefficient is 0.8. For a thermoelastic problem, one can tailor the variation of either the shear modulus or the thermal expansion coefficient to achieve a given stress state in a uniformly heated rotating disk. We have not considered the case of tailoring both the shear modulus and the coefficient of thermal expansion to achieve the desired stress state in the disk.

## 6. Conclusions

For a rotating hollow circular disk with the thickness, the mass density, the thermal expansion coefficient and the shear modulus given by power-law functions of the radius, we have given exact solutions for stresses, the hydrostatic pressure and the radial displacement. The analytical solution is also provided for the case of the shear modulus varying exponentially but constant disk thickness, thermal expansion coefficient and mass density for both hollow and solid disks. When the shear modulus, thermal expansion coefficient, mass density and the thickness of hollow or solid disks are arbitrary smooth functions of the radius, the problem is solved numerically by the differential quadrature method. It is found from numerical results for some example problems that fixing the inner surface of a hollow disk considerably reduces the peak hoop stress but increases the maximum radial stress. For a fixed-free hollow disk, the maximum radial stress is greater than the maximum hoop stress but the reverse holds for a free-free hollow disk. Improper gradation of the shear modulus, the disk thickness and the mass density can increase the maximum radial and hoop stresses as compared to their values for a homogeneous disk of constant thickness. In a uniformly heated FG rotating disk, the radial stress is tensile (compressive) if the thermal expansion coefficient increases (decreases) with the radius, and the magnitude of the hoop stress is maximum at a point on the inner surface of the disk.

We have also analyzed the material tailoring problem of finding the radial variation of the shear modulus or the thermal expansion coefficient to achieve a constant value of either the hoop stress or the in-plane shear stress or a linear combination of the radial and the hoop stresses. For a rotating annular disk, we present the explicit expression for the variation of the thermal expansion coefficient to achieve uniform hoop stress in the disk. For a rotating solid disk, we give the exact expressions for the shear modulus and thermal expansion coefficient as functions of the radius for the hoop stress to be constant in the disk.

The present results should serve as benchmarks for comparison with those computed using numerical algorithms.

## Acknowledgements

This work was partially supported by the Office of Naval Research grant N00014-06-1-0567 to Virginia Polytechnic Institute and State University with Dr. Y. D. S. Rajapakse as the program manager. Views expressed in the paper are those of authors, and neither of the funding agency nor of their institutions.

## References

- [1] Roesler J, Paulino G, Gaedike C, Bordelon A, Park K. Fracture behavior of functionally graded concrete materials for rigid pavements. *J Transport Res Board* 2007;2037:40–9.
- [2] Lucignano C, Quadri F. Indentation of functionally graded polyester composites. *Measurement* 2009;42:894–902.
- [3] Chakraborty A, Dutta AK, Ray KK, et al. An effort to fabricate and characterize in-situ formed graded structure in a ceramic-metal system. *J Mater Process Technol* 2009;209(5):2681–92.
- [4] Bilgili E. Controlling the stress-strain inhomogeneities in axially sheared and radially heated hollow rubber tubes via functional grading. *Mech Res Commun* 2003;30:257–66.
- [5] Bilgili E. Functional grading of rubber tubes within the context of a molecularly inspired finite thermoelastic model. *Acta Mech* 2004;169:79–85.
- [6] Bilgili E. Modelling mechanical behavior of continuously graded vulcanized rubbers. *Plast Rubber Compos* 2004;33(4):163–9.
- [7] Marzocca AJ. Finite element analysis of cure in a rubber cylinder. *Polymer* 1991;32:1456–60.
- [8] Azaar K, Lamine B, Granger R, Rosca ID, Vergnaud JM. Process of cure of ethylene-propylene diene monomer rubbers – evaluation of state of cure. *Plast Rubber Compos* 2000;29:253–7.
- [9] Gillen KT, Terrill ER, Winter RM. Modulus mapping of rubbers using micro- and nano-indentation techniques. *Rubber Chem Technol* 2001;74:428–50.
- [10] Timoshenko SP, Goodier JN. *Theory of elasticity*. 3rd ed. New York: McGraw-Hill; 1970.
- [11] Horgan CO, Chan AM. The stress response of functionally graded isotropic linearly elastic rotating disks. *J Elast* 1999;55:219–30.
- [12] Jahed H, Farshi B, Bidabadi J. Minimum weight design of inhomogeneous rotating discs. *Int J Press Vessels Pip* 2005;82:35–41.
- [13] Eraslan AN, Akis T. On the plane strain and plane stress solutions of functionally graded rotating solid shaft and solid disk problems. *Acta Mech* 2006;181:43–63.
- [14] Kordkheili SAH, Naghdabadi R. Thermoelastic analysis of a functionally graded rotating disk. *Compos Struct* 2007;79:508–16.
- [15] You LH, You XY, Zhang JJ, et al. On rotating circular disks with varying material properties. *Z Angew Math Phys* 2007;58:1068–84.
- [16] Hojjati MH, Jafari S. Semi-exact solution of elastic non-uniform thickness and density rotating disks by homotopy perturbation and Adomian's decomposition methods Part I: elastic solution. *Int J Press Vessels Pip* 2008;85:871–8.
- [17] Bayat M, Saleem M, Sahari BB, et al. Analysis of functionally graded rotating disks with variable thickness. *Mech Res Commun* 2008;35:283–309.
- [18] Bayat M, Saleem M, Sahari BB, et al. Mechanical and thermal stresses in a functionally graded rotating disk with variable thickness due to radially symmetry loads. *Int J Press Vessels Pip* 2009;86:357–72.
- [19] Bayat M, Sahari BB, Saleem M, et al. Thermoelastic solution of a functionally graded variable thickness rotating disk with bending based on the first-order shear deformation theory. *Thin Wall Struct* 2009;47:568–82.
- [20] Bayat M, Sahari BB, Saleem M, et al. Bending analysis of a functionally graded rotating disk based on the first order shear deformation theory. *Appl Math Model* 2009;33:4215–30.
- [21] Vullo V, Vivio F. Elastic stress analysis of non-linear variable thickness rotating disks subjected to thermal load and having variable density along the radius. *Int J Solids Struct* 2008;45:5337–55.
- [22] Vivio F, Vullo V. Elastic stress analysis of rotating converging conical disks subjected to thermal load and having variable density along the radius. *Int J Solids Struct* 2007;44:7767–84.
- [23] Zenkour AM. Stress distribution in rotating composite structures of functionally graded solid disks. *J Mater Process Technol* 2009;209:3511–7.
- [24] Zenkour AM. Elastic deformation of the rotating functionally graded annular disk with rigid casing. *J Mater Sci* 2007;42:9717–24.
- [25] Batra RC. Finite plane strain deformations of rubberlike materials. *Int J Numer Methods Eng* 1980;15(1):145–60.
- [26] Batra RC. Optimal design of functionally graded incompressible linear elastic cylinders and spheres. *AIAA J* 2008;46(8):2050–7.
- [27] Batra RC, Iaccarino GL. Exact solutions for radial deformations of a functionally graded isotropic and incompressible second-order elastic cylinder. *Int J Non Linear Mech* 2008;43:383–98.
- [28] Batra RC, Bahrami A. Inflation and eversion of functionally graded non-linear elastic incompressible circular cylinders. *Int J Non Linear Mech* 2009;44:311–23.
- [29] Bilgili E, Bernstein B, Arastoopour H. Inhomogeneous shearing deformation of a rubber-like slab within the context of finite thermoelasticity with entropic origin for the stress. *Int J Non Linear Mech* 2001;36:887–900.
- [30] Bilgili E, Bernstein B, Arastoopour H. Effect of material non-homogeneity on the inhomogeneous shearing deformation of a Gent slab subjected to a temperature gradient. *Int J Non Linear Mech* 2003;38:1351–68.
- [31] Shu C. *Differential quadrature and its application in engineering*. London: Springer; 2000.
- [32] Leissa W, Vagins M. The design of orthotropic materials for stress optimization. *Int J Solids Struct* 1978;14:517–26.
- [33] Qian LF, Batra RC. Design of bidirectional functionally graded plate for optimal natural frequencies. *J Sound Vibration* 2005;280:415–24.
- [34] Batra RC, Vidoli S. Higher order piezoelectric plate theory derived from a three-dimensional variational principle. *AIAA J* 2002;40:91–104.
- [35] Batra RC, Jin J. Natural frequencies of a functionally graded rectangular plate. *J Sound Vibration* 2005;282:509–16.
- [36] Batra RC. Torsion of a functionally graded cylinder. *AIAA J* 2006;44:1363–5.
- [37] Batra RC. Higher order shear and normal deformable theory for functionally graded incompressible linear elastic plates. *Thin Walled Struct* 2007;45:974–82.
- [38] Aimmanee S, Batra RC. Analytical solution for vibration of an incompressible isotropic linear elastic rectangular plate, and frequencies missed in previous solutions. *J Sound Vibration* 2007;302:613–20.
- [39] Zimmerman RW, Lutz MP. Thermal stresses and thermal expansion in a uniformly heated functionally graded cylinder. *J Therm Stress* 1999;22:177–88.
- [40] Batra RC. *Elements of continuum mechanics*. Reston: AIAA; 2005.